HHS Public Access

Author manuscript

J Pediatr Surg. Author manuscript; available in PMC 2023 January 01.

Published in final edited form as:

J Pediatr Surg. 2022 January ; 57(1): 26–33. doi:10.1016/j.jpedsurg.2021.09.015.

A Pumpless Artificial Lung without Systemic Anticoagulation: The Nitric Oxide Surface Anticoagulation System

Brian P Fallon[1], **Orsolya Lautner-Csorba**[1], **Alex J Thompson**[1], **Gergely Lautner**[1], **Adrianna Kayden**[1], **Matthew D Johnson**[1], **Stephen L Harvey**[1], **Mark W Langley**[1], **Alvaro Rojas Peña**[1], **Robert H Bartlett**[1], **Ronald B Hirschl**[1,2]

[1]Extracorporeal Life Support Laboratory, Department of Surgery, Michigan Medicine, Ann Arbor, Michigan, USA

[2]Department of Surgery, Section of Pediatric Surgery, Michigan Medicine, Ann Arbor, Michigan, USA

Abstract

Background: Artificial lungs have the potential to serve as a bridge to transplantation or recovery for children with end-stage lung disease dependent on extracorporeal life support, but such devices currently require systemic anticoagulation. We describe our experience using the novel Nitric Oxide (NO) Surface Anticoagulation (NOSA) system—an NO-releasing circuit with NO in the sweep gas—with the Pediatric MLung—a low-resistance, pumpless artificial lung.

Methods: NO flux testing: MLungs (n=4) were tested using veno-venous extracorporeal life support in a sheep under anesthesia with blood flow set to 0.5 and 1 L/min and sweep gas blended with 100 ppm NO at 1, 2, and 4 L/min. NO and NO_2 were measured in the sweep and exhaust gas to calculate NO flux across the MLung membrane.

Pumpless implants: Sheep (20–100 kg, n=3) underwent thoracotomy and cannulation via the pulmonary artery (device inflow) and left atrium (device outflow) using cannulae and circuit components coated with an NO donor (diazeniumdiolated dibutylhexanediamine; DBHD-N_2O_2) and argatroban. Animals were connected to the MLung with 100 ppm NO in the sweep gas under anesthesia for 24 hours with no systemic anticoagulation after cannulation.

Results: NO flux testing: NO flux averaged 3.4±1.0 flux units ($x10^{-10}$ mol/cm^2/min) (human vascular endothelium: 0.5–4 flux units).

Pumpless implants: 3 sheep survived 24 hours with patent circuits. MLung blood flow was 716±227 mL/min. Outlet oxygen saturation was 98.3±2.6%. Activated clotting time was 151±24 seconds. Platelet count declined from 334,333±112,225 to 123,667±7,637 over 24 hours. Plasma free hemoglobin and leukocyte and platelet activation did not significantly change.

Corresponding author: Brian P Fallon, ECLS Laboratory, Department of Surgery, Michigan Medicine, B560 MSRB II/SPC 5686, 1150 W. Medical Center Drive, Ann Arbor, MI 48109, USA, **Corresponding author telephone:** 734-615-5357, bfallon@med.umich.edu.

Conclusions: The NOSA system provides NO flux across a gas-exchange membrane of a pumpless artificial lung at a similar rate as native vascular endothelium and achieves effective local anticoagulation of an artificial lung circuit for 24 hours.

Keywords

artificial lung; non-thrombogenic circuits; biocompatibility; extracorporeal life support; extracorporeal membrane oxygenation; pediatric respiratory failure

Introduction

Pediatric patients with end-stage lung disease dependent on extracorporeal life support (ECLS) face few options for recovery. Pumpless artificial lungs can be a cheaper, more portable alternative to a complicated ECLS circuit. These would serve as a bridge to lung transplantation or recovery that allow patients to ambulate and participate in rehabilitation. Any form of extracorporeal support is associated with a high risk of hemorrhagic and thrombotic complications [1] and pumpless artificial lungs are no exception. Cases of long-term support with commercial oxygenators used as pumpless artificial lungs for pediatric patients with respiratory failure and pulmonary hypertension have been complicated by intracranial hemorrhage and ischemic stroke [2, 3]. Progress in artificial-lung design has led to incremental improvements in biocompatibility by reducing device size, optimizing pumpless operation, and modifying blood flow paths to eliminate stagnation points and areas of high shear [4]. Despite these advancements, systemic anticoagulation is still necessary to prevent rapid and definitive circuit failure.

Much research has been done in search of a biocompatible blood-contacting surface that would eliminate the need for systemic anticoagulation, allowing for safer, longer-term use of extracorporeal circuits [5–9]. One approach is to mimic the native endothelium by releasing nitric oxide (NO) at the site of blood contact. NO inhibits platelet and cellular activation and has an extremely short half-life in the blood, confining its effects to the local environment of the circuit. We have developed a circuit coating containing diazeniumdiolated dibutylhexanediamine (DBHD-N_2O_2), which elutes NO when in contact with blood, and an immobilized direct thrombin inhibitor, argatroban, which prevents fibrin formation [10, 11]. This coating is not compatible with gas exchange in the hollow-fiber membrane lungs commonly used in ECLS. To account for the thrombogenic surface within the membrane lung itself, NO can be delivered directly to the fiber surfaces as part of the sweep gas. Using these two modalities, we have developed the NO Surface Anticoagulation (NOSA) system to achieve biocompatibility in extracorporeal circuits based on local NO delivery. The NOSA system has two components: (1) DBHD-N_2O_2/argatroban surface coating applied to all tubing, connectors, and cannulae and (2) NO blended into the sweep gas delivered to the hollow-fiber membrane lung. Previous studies have demonstrated the effectiveness of the DBHD-N_2O_2/argatroban coating at maintaining patency of an arteriovenous shunt in rabbits [10, 11]. Electrochemically generated NO delivered in the sweep gas into a membrane lung limits leukocyte activation in cardiopulmonary bypass [12] and platelet activation in neonatal ECLS animal models [13], but its level of NO delivery to the blood-contacting surface of the membrane in vivo has yet to be demonstrated. Similarly,

the ability of a system based on NO delivery to prevent thrombosis of a complete ECLS circuit remains unproven.

Here, we apply the NOSA system to a circuit containing the Pediatric MLung [4, 14], a low-resistance, implantable, pumpless artificial lung specifically designed for long-term support of pediatric patients. First, the level of NO flux across the hollow-fiber membrane of the Pediatric MLung into the blood is quantified while the device is connected to a controlled veno-venous (V-V) ECLS circuit and receives NO from an electrochemical NO generator (NOgen) in an ovine model. Subsequently, the complete NOSA system (circuit coating and NOgen) is tested for 24 hours without anticoagulation in the Pediatric MLung implanted in its intended pumpless configuration. We hypothesized that NO would be released at physiologic levels by the Pediatric MLung membrane and from the DBHD-N_2O_2/argatroban surface coating. Additionally, we hypothesized that the NOSA system would prevent thrombosis of the pumpless artificial lung circuit without systemic anticoagulation.

Methods

All animal experiments were performed following the National Institutes of Health's Guide for the Care and Use of Laboratory Animals. This study was approved by the University Committee on Use and Care of Animals (UCUCA) at the University of Michigan.

Nitric Oxide Surface Anticoagulation (NOSA) System

NO generator (NOgen): NO gas was generated by electrochemical reduction of 1 M sodium nitrite solution with Cu(II)-1,4,7-trimethyl-1,4,7-triazacyclononane mediator on open cell carbon foam electrode, and extracted into a nitrogen gas stream (50–200 mL/min) using a silicone hollow fiber gas separator membrane (PermSelect PDMSX-2.1, Ann Arbor, MI) and injected into the sweep gas of the MLung. The current for generating 100 ppm NO within the sweep gas was feedback controlled by monitoring the NO level in the sweep gas with electrochemical sensors (AlphaSense, Essex, United Kingdom).

Circuit coating: All the cannulae and circuit components were prepared using a combined coating method previously reported [10]. Briefly, the interior polymer surfaces (circuit tubing: polyvinylchloride (PVC), connectors: polycarbonate (PC), cannulae: wire-reinforced polyurethane) were coated individually with triple layers. The first two polymer layers were NO donor layers with 25 wt% diazeniumdiolated dibutylhexanediamine (DBHD-N_2O_2) and 10 wt% poly(lactic-co-glycolic acid) (PLGA, Sigma-Aldrich, St. Louis, MO) additive. The third, top layer consisted of 10 uM argatroban (Toronto Research Chemicals, Toronto, Canada). The polymer media for the NO coating was CarboSil (co-polymer) dissolved in tetrahydrofuran (THF, Sigma-Aldrich, St. Louis, MO), and CarboSil/HMDI (hexamethylene diisocyanate, Sigma-Aldrich, St. Louis, MO) in THF for argatroban.

Pediatric MLung

The Pediatric MLung is a novel artificial lung specifically designed for pediatric patients [4, 14]. It achieves low resistance with dual blood inlets and a custom low-density polymethylpentene fiber mat. Gas-exchange efficiency is optimized with concentric gates

that create swirling blood flow paths to disrupt the boundary layer. The gas exchange and relevant sizing characteristics of the device are given in Table 1.

For both the NO flux testing and pumpless implants with NOSA, the Pediatric MLung was primed with sterile technique with Plasma-Lyte (Baxter International, Deerfield, IL) prewarmed to 37°C. The MLung was then connected to the inflow cannula and forward bled to flush the Plasma-Lyte and ensure no residual air bubbles. The outflow cannula was subsequently connected.

NO Flux Testing in Pediatric MLungs

NO flux testing on 4 Pediatric MLungs was performed in a healthy sheep receiving systemic anticoagulation. The primary outcome was the amount of NO released per square centimeter of MLung membrane surface area.

Surgical procedure: The sheep (60 kg) was anesthetized with intravenous propofol 7 mg/kg, intubated, and mechanically ventilated. General anesthesia was maintained with inhaled isoflurane 1–3.5%. An arterial line was placed in the right femoral artery and the animal was cannulated for V-V ECLS. The veno-venous circuit consisted of 24-Fr right femoral vein drainage (Medtronic, Minneapolis, MN), 19-Fr right jugular vein reinfusion (Medtronic, Minneapolis, MN), 1/4-inch and 3/8-inch PVC tubing (TYGON, Saint-Gobain Performance Plastic, Wayne, NJ), a non-occlusive roller pump (developed in-house), and the Pediatric MLung. The circuit components were not coated with DBHD-N_2O_2/argatroban. Prior to cannulation, an initial bolus of 100 units/kg of sodium heparin (Fresenius Kabi, Lake Zurich, IL) was used with continued administration to maintain systemic anticoagulation with activated clotting time (ACT) targets of 240–280 seconds throughout the experiment. Prior to connection, methylprednisolone 500 mg (Pfizer, New York, NY) was administered to limit the systemic inflammatory reaction to the Pediatric MLung.

Circuit settings: Circuit blood flows of 0.5 and 1 L/min were tested at sweep rates of 1, 2, and 4 L/min. The sweep gas contained 97% O_2 and 3% CO_2 with 100 ppm NO delivered by the NOgen. This NO concentration was chosen based on previous preliminary work in our lab (unpublished) that demonstrated efficacy of this concentration for preventing thrombosis.

NO flux measurement: Each setting was allowed to stabilize for 3–5 minutes at which point NO and NO_2 values in the sweep (NO_{in}/$NO_{2,in}$) and exhaust gas (NO_{out}/$NO_{2,out}$) were measured with electrochemical sensors (AlphaSense, Essex, United Kingdom). NO flux was calculated using the following formula.

$$NO\ flux\left[\frac{mol}{min \cdot cm^2}\right] = \frac{101,325[Pa] \cdot \left(NO_{in}[ppm] - NO_{out}[ppm] - NO_{2,out}[ppm] + NO_{2,in}[ppm]\right) \cdot 10-6\left[\frac{1}{ppm}\right] \cdot F\left[\frac{L}{min}\right] \cdot 10^{-3}\left[\frac{L}{m^3}\right]}{8.314\left[\frac{m^3 Pa}{molK}\right] \cdot 298.15[K] \cdot A\left[cm^2\right]}$$

The target range for NO flux across the MLung membrane was considered 0.5–4 flux units, equal to the range of NO release by native human vascular endothelium [15].

Pumpless Implants with NOSA

Pediatric MLungs were implanted in 3 healthy sheep with no systemic anticoagulation. The primary outcome was circuit patency with no thrombosis for 24 hours.

Circuit construction and sterilization: The circuit consisted of the pre-lung circuitry with two 12-cm long 3/8-inch PVC tubing segments (TYGON, Saint-Gobain Performance Plastic, Wayne, NJ) and a 3/8-inch PC luer-lock connector, and the post-lung circuitry with a 12-cm long 5/16-inch PVC tubing segment (TYGON, Saint-Gobain Performance Plastic, Wayne, NJ) and a 3/8-inch PC luer-lock connector. The circuit was coated with DBHD-N_2O_2/argatroban as above. After the coating process, the circuit components (connectors and tubing) were adhered together with Carbosil/THF solution. The circuit was then allowed to dry under a fume hood at room temperature for 2 days and stored at 4°C until used. The circuit was sterilized the day of the implant procedure with ortho-Phthalaldehyde solution (Metricide OPA Plus, Metrex Research, Romulus, MI) per manufacturer instruction.

Surgical procedure: Three healthy sheep (20–100 kg) were anesthetized with intravenous propofol 7 mg/kg, intubated, and mechanically ventilated. General anesthesia was maintained with inhaled isoflurane 1–3.5%. Intravascular monitoring lines were placed in the left carotid artery (arterial line) and the right jugular vein (central venous line and pulmonary artery catheter) under general inhaled anesthesia and connected to pressure transducers for continuous monitoring. A 14–16-mm ultrasonic perivascular flow probe (Transonic, Ithaca, NY) was placed on the aorta for measurement of cardiac output (CO). Prior to vascular access, the animals received a bolus of 100 units/kg sodium heparin (Fresenius Kabi, Lake Zurich, IL) and methylprednisolone 500 mg (Pfizer, New York, NY) to limit systemic inflammatory reaction to the artificial lung. The Pediatric MLung was implanted via a left thoracotomy using the pulmonary artery (PA) for device inflow and the left atrium (LA) for device outflow. For the PA cannulation, a 10-mm ringed polytetrafluoroethylene (PTFE) vascular graft (Gore Medical, Newark, DE) was sewn to the main PA in an end-to-side fashion and a 28-Fr single-stage venous cannula (Medtronic DLP, Minneapolis, MN) with the tip removed was inserted through the graft to the level of the anastomosis. For the LA cannulation, concentric purse-string sutures were placed in the LA and a 28-Fr single-stage venous cannula (Medtronic DLP, Minneapolis, MN) was passed through a 10-mm PTFE graft and 2–3 cm into the LA. The purse-string sutures were tightened and the graft was secured to the LA and the cannula. The cannulae were flushed with a combined total of 40 mL of normal saline containing 400 units of heparin. The MLung was connected to the PA cannula and blood primed as described above. The MLung blood outlet was then connected to the LA cannula and full circuit flow initiated (Figure 1). The NOgen was connected to the sweep gas inlet of the Pediatric MLung. Target NO concentration in the sweep gas was 100 ppm as in the NO flux testing. The animals were maintained under general anesthesia and full mechanical ventilation for 24 hours of Pediatric MLung support. After Pediatric MLung attachment, the sheep received no additional heparin

throughout the duration of the study. Details of data collection for these experiments can be found in Table 2.

Circuit NO release measurement: The NO flux from the coated circuits was measured the day before initiation of each pumpless implant experiment and the day after the end of each experiment (after 24 hours of blood exposure) via an ozone chemiluminescent NO Analyzer (NOA, GE Sievers 280i Nitric Oxide Analyzer, Boulder, CO). In summary, a 0.5-cm sample of the circuit tube was placed in 5 mL phosphate buffered saline at 37°C. NO was continuously purged out from the bathing solution with a nitrogen sweep with a 200 mL/min flow rate and measured from the headspace of the NOA cell (ca. 5.6 Torr chamber pressure, ca. 6 psi oxygen pressure).

Data Analysis

Descriptive statistics alone are reported for the NO flux testing and pumpless implants with NOSA due to small sample size and limited power to detect statistically significant differences between experimental settings and timepoints.

Results

NO Flux Testing in Pediatric MLungs

For the NO flux testing in the Pediatric MLung, NO flux averaged 3.4±1.0 flux units ($x10^{-10}$ mol/cm^2/min) across all settings and all devices (Figure 2). All settings in all devices produced NO flux levels within the target range of 0.5–4 flux units, which is the estimated normal range for NO release by human vascular endothelium [15].

Pumpless Implants with NOSA

Three sheep survived 24 hours of support with a patent circuit and no thrombotic complications. Animal hemodynamics, acid/base balance, PA pressures, and CO were maintained within normal physiological parameters (Table 3). Three sheep were excluded due to flaws in MLung construction: 2 devices had leaks in the silicone potting that separates the blood from the sweep gas, resulting in massive air embolus into the left atrium, and 1 device had foreign material inside the fibers, resulting in rapid thrombosis of the MLung.

MLung blood flow was 716±227 mL/min (Figure 3A) or 22.6±9.1% of CO across the 24-hour period. Pressure drop across the MLung was 6.3±2.9 mmHg (Figure 3A), equating to a calculated MLung resistance of 10.2±7.4 mmHg/L/min (Figure 3B). MLung outlet oxygen saturation was 98.3±2.6% (Figure 3C) compared to an inlet saturation of 75.3±12.5%.

Mean ACT was 151±24 seconds. None of 39 ACTs collected after MLung connection were within or above the target range for therapeutic anticoagulation for these sheep (240–280 seconds) (Figure 4). Initial elevation in ACT was due to heparinization of the animal at the time of vascular access and cannulation.

Hemoglobin and white blood cell count remained stable from baseline to the end of the experiments (Figures 5A and 5B). Platelet counts declined from 334,333±112,225 at

baseline to 123,667±7,637 at 24 hours (Figure 5C), though all counts remained above 100,000. Plasma free hemoglobin decreased during the 24 hours and stayed well below 50 mg/dL, the Extracorporeal Life Support Organization definition for hemolysis (Figure 5D). Flow cytometry results demonstrated a mild increase in P-selectin expression to 110±23% of baseline and in granulocyte-specific CD11b to 119±28% of baseline after 24 hours (Figure 6). Expression of lymphocyte- and monocyte-specific CD11b did not increase. Descriptive statistics alone were used for laboratory values at hours 0 and 24 due to low sample size.

Methemoglobin, an indicator of NO toxicity, averaged 1.7±0.4% of total hemoglobin for the 3 animals across the 24-hour experiment. The normal range is 0–3%.

The average NO flux from the coated circuit components was 1.1±0.1 flux units before blood exposure and 0.9±0.5 flux units after 24 hours of blood exposure. A representative MLung and circuit at the end of an experiment is shown in Figure 7, demonstrating minimal clot burden. The narrow rings of thrombus at the end of most tubing segments correspond to the locations of connector insertion.

Discussion

This study is the first to show effective circuit-based anticoagulation of a pumpless artificial-lung circuit, eliminating the need for systemic anticoagulation. The NOSA system produced NO flux within a physiologic range of 0.5–4 flux units at all blood-contacting surfaces of the MLung circuit. Electrochemically generated NO was blended into the sweep gas going to the MLung to effectively deliver NO across the hollow-fiber membrane without affecting gas exchange. The remainder of the circuit components were coated with an NO-releasing molecule (DBHD-N_2O_2) as well as argatroban. This level of NO release by the NOSA system maintained circuit patency and prevented thrombosis during 24 hours of MLung support without the use of systemic anticoagulation. This was also associated with minimal platelet and leukocyte activation.

The goal in developing the Pediatric MLung is to create a simpler form of long-term support for children with lung failure who are stranded on ECLS. We now know that the lung is capable of remodeling and recovery from severe disease, though this process can take months [2, 16–19]. Those patients with end-stage lung disease for whom recovery is not an option typically spend over 100 days on the transplant list [20]. The cost and complexity of ECLS make it a poor option for the long-term support these patients need [21–23]. An implantable artificial lung like the Pediatric MLung would be simpler, cheaper, and more portable than the current ECLS systems. The Pediatric MLung takes advantage of the pressure gradient between the PA and LA to eliminate the need for a pump. Central cannulation provides added cannula stability, which allows for safe wakefulness and ambulation [24]. This would facilitate rehabilitation and overall improved quality of life for these patients as they await lung recovery or transplantation [24–26].

Despite the benefits of artificial lungs for long-term support, longer extracorporeal support is associated with an increase in device-related complications [27]. Additionally, hemorrhagic and thrombotic complications have occurred at high rates in the limited published

experience with pumpless artificial lungs in children [2, 3]. Non-thrombogenic circuits such as the NOSA system could improve the biocompatibility of these devices and, ideally, would allow them to be used safely without the need for long-term anticoagulation.

Many approaches have been taken to improve the biocompatibility of circuits, including applying coatings of inert hydrophilic molecules [5], immobilized proteins [28], and even cultured endothelial cells [8]. Circuits in clinical use are commonly coated with heparin. This has been shown to reduce the dose of anticoagulation required to maintain circuit patency [6]; however, these circuits cannot be operated reliably and safely without anticoagulation. Furthermore, heparin coating has been shown to confer a risk of heparin-induced thrombocytopenia—a rare but serious complication of heparin use [6]. NO release is an ideal mechanism for circuit biocompatibility because it mimics the physiology of the native vascular endothelium, which relies on NO to prevent platelet activation [29]. The physiologic level of NO flux has been shown to be 0.5–4 flux units [15], making this a logical initial target for an NO-releasing circuit. Argatroban added to the DBHD-N_2O_2 coating has previously been shown to further reduce thrombus formation compared to DBHD-N_2O_2 alone [11]. The current study has demonstrated that the DBHD-N_2O_2/argatroban coating releases NO at physiologic levels throughout 24 hours of blood exposure. Electrochemically generated NO at 100 ppm can be effectively delivered in the sweep gas and also produces physiologic levels of NO flux across the hollow-fiber polymethylpentene membranes. Importantly, unlike other methods of coating fibers of membrane lungs [9], this method of NO delivery in the sweep gas does not affect the gas-exchange performance of the artificial lung. The pumpless implant studies demonstrate that the NO flux levels produced by the NOSA system do appear adequate to maintain patency of an artificial lung circuit without thrombotic complications. There was a decline in platelet counts in each of the 3 animals in the pumpless implant experiments, suggesting that the NOSA system may not completely ameliorate the platelet consumption commonly associated with ECLS initiation. However, platelet counts remained above the safe level of 100,000, likely not resulting in coagulopathy. Nevertheless, the recovery of platelet counts and the trend in platelet activation will be important to understand over future longer-term studies of the MLung with the NOSA system.

The primary limitation of this study is the small sample size for the pumpless implant experiments and lack of a comparison group. As a result, this study is not powered to identify statistically significant changes in sheep data and laboratory analyses over the course of the experiment, nor to compare these outcomes to a similar model using systemic anticoagulation. As a pilot study, this demonstrates the feasibility of achieving the primary outcome of Pediatric MLung circuit patency without thrombotic complications over 24 hours using the NOSA system. Future studies will increase the duration of support with the NOSA system and include comparisons to anticoagulated controls. Another consideration is the variation in the size of the animals used. This resulted in a variation in CO and resultant absolute device flow; however, the goal of these studies was to evaluate the biocompatibility of the NOSA system, which is unlikely to be affected by the weight of the experimental subject within the same species. In previous studies, we have demonstrated successful use of the Pediatric MLung in a 7-day pediatric sheep model, with sheep weighing 12–20 kg (publication forthcoming). Though the Pediatric MLung has not yet been tested in a neonatal

animal model, the NOSA system has been shown to be effective for ECLS in a premature sheep model (publication forthcoming). The next step for this work will be to evaluate the longer-term performance of the NOSA system with the Pediatric MLung in this seven-day pediatric sheep model.

In conclusion, this study demonstrates that the NOSA system provides physiologic levels of NO flux to a pumpless artificial lung circuit. This level of NO release achieves effective local anticoagulation of the artificial lung circuit for 24 hours. This represents a major step in the development of a biocompatible circuit for pediatric pumpless artificial lungs that can also be translated to other forms of extracorporeal support. The implementation of an effective surface-based anticoagulation system such as the NOSA system could cause a paradigm shift in extracorporeal circulation and lead to safe, long-term use of pumpless artificial lungs as a bridge to lung transplantation or recovery for children with lung failure.

Acknowledgements

We would like to thank Joseph Hill for performing much of the laboratory testing for this manuscript.

Abbreviations:

(ACT)	activated clotting time
(CO)	cardiac output
(DBHD-N_2O_2)	diazeniumdiolated dibutylhexanediamine
(ECLS)	extracorporeal life support
(LA)	left atrium
(NO)	nitric oxide
(NOgen)	nitric oxide generator
(NOSA)	Nitric Oxide Surface Anticoagulation
(PC)	polycarbonate
(PTFE)	polytetrafluoroethylene
(PVC)	polyvinylchloride
(PA)	pulmonary artery

References

[1]. Extracorporeal Life Support Organization International Summary. 2020.

[2]. Hoganson DM, Gazit AZ, Boston US, Sweet SC, Grady RM, Huddleston CB, et al. Paracorporeal lung assist devices as a bridge to recovery or lung transplantation in neonates and young children. J Thorac Cardiovasc Surg 2014;147(1):420–7. [PubMed: 24199759]

[3]. Strueber M, Hoeper MM, Fischer S, Cypel M, Warnecke G, Gottlieb J, et al. Bridge to Thoracic Organ Transplantation in Patients with Pulmonary Arterial Hypertension Using a Pumpless Lung Assist Device. Am J Transplant 2009;9(4):853–7. [PubMed: 19344471]

[4]. Thompson AJ, Buchan S, Carr B, Poling C, Hayes M, Fernando UP, et al. Low-Resistance, Concentric-Gated Pediatric Artificial Lung for End-Stage Lung Failure. ASAIO J 2020;66(4):423–32. [PubMed: 31192843]

[5]. Lorusso R, De Cicco G, Totaro P, Gelsomino S. Effects of phosphorylcholine coating on extracorporeal circulation management and postoperative outcome: a double-blind randomized study. Interact Cardiovasc Thorac Surg 2008;8(1):7–11. [PubMed: 18728037]

[6]. Biran R, Pond D. Heparin coatings for improving blood compatibility of medical devices. Advanced Drug Delivery Reviews 2017;112:12–23. [PubMed: 28042080]

[7]. Ukita R, Wu K, Lin X, Carleton NM, Naito N, Lai A, et al. Zwitterionic poly-carboxybetaine coating reduces artificial lung thrombosis in sheep and rabbits. Acta biomaterialia 2019;92:71–81. [PubMed: 31082571]

[8]. Klein S, Hesselmann F, Djeljadini S, Berger T, Thiebes AL, Schmitz-Rode T, et al. EndOxy: Dynamic Long-Term Evaluation of Endothelialized Gas Exchange Membranes for a Biohybrid Lung. Annals of Biomedical Engineering 2020;48(2):747–56. [PubMed: 31754901]

[9]. Roberts TR, Choi JH, Wendorff DS, Harea GT, Beely BM, Sieck KN, et al. Tethered Liquid Perfluorocarbon Coating for 72 Hour Heparin-Free Extracorporeal Life Support. ASAIO J 2021.

[10]. Major TC, Brant DO, Reynolds MM, Bartlett RH, Meyerhoff ME, Handa H, et al. The attenuation of platelet and monocyte activation in a rabbit model of extracorporeal circulation by a nitric oxide releasing polymer. Biomaterials 2010;31(10):2736–45. [PubMed: 20042236]

[11]. Major TC, Brisbois EJ, Jones AM, Zanetti ME, Annich GM, Bartlett RH, et al. The effect of a polyurethane coating incorporating both a thrombin inhibitor and nitric oxide on hemocompatibility in extracorporeal circulation. Biomaterials 2014;35(26):7271–85. [PubMed: 24927680]

[12]. Qin Y, Zajda J, Brisbois EJ, Ren H, Toomasian JM, Major TC, et al. Portable Nitric Oxide (NO) Generator Based on Electrochemical Reduction of Nitrite for Potential Applications in Inhaled NO Therapy and Cardiopulmonary Bypass Surgery. Molecular Pharmaceutics 2017;14(11):3762–71. [PubMed: 29020775]

[13]. Rossidis AC, Lawrence KM, Mejaddam AY, Kim AG, Baumgarten HD, Coons BE, et al. The Effects of Nitric Oxide in Oxygenator Sweep Gas During Extracorporeal Circulation in a Neonatal Ovine Model. ASAIO J 2020;66(6):671–6. [PubMed: 31335368]

[14]. Fernando UP, Thompson AJ, Potkay J, Cheriyan H, Toomasian J, Kaesler A, et al. A Membrane Lung Design Based on Circular Blood Flow Paths. ASAIO J 2017;63(5):637–43. [PubMed: 28665829]

[15]. Vaughn MW, Kuo L, Liao JC. Estimation of nitric oxide production and reaction rates in tissue by use of a mathematical model. Am J Physiol 1998;274(6 Pt 2):H2163–76. [PubMed: 9841542]

[16]. Deanda A, Cahill JL, Bernstein D, Starnes VA, Reitz BA. Elective transplant pneumonectomy. J Pediatr Surg 1998;33(4):655–6. [PubMed: 9574774]

[17]. Green TP, Moler FW, Goodman DM. Probability of survival after prolonged extracorporeal membrane oxygenation in pediatric patients with acute respiratory failure. Crit Care Med 1995;23(6):1132–9. [PubMed: 7774227]

[18]. Brogan TV, Zabrocki L, Thiagarajan RR, Rycus PT, Bratton SL. Prolonged extracorporeal membrane oxygenation for children with respiratory failure. Pediatr Crit Care Med 2012;13(4):e249–e54. [PubMed: 22596069]

[19]. Nelson-McMillan K, Vricella LA, Stewart FD, Young J, Shah AS, Hibino N, et al. Recovery from Total Acute Lung Failure After 20 Months of Extracorporeal Life Support. ASAIO J 2020;66(1):e11–e4. [PubMed: 30908288]

[20]. Lancaster TS, Miller JR, Epstein DJ, DuPont NC, Sweet SC, Eghtesady P. Improved waitlist and transplant outcomes for pediatric lung transplantation after implementation of the lung allocation score. J Heart Lung Transplant 2017;36(5):520–8. [PubMed: 27866928]

[21]. Faraoni D, Nasr VG, DiNardo JA, Thiagarajan RR. Hospital Costs for Neonates and Children Supported with Extracorporeal Membrane Oxygenation. J Pediatr 2016;169:69–75.e1. [PubMed: 26547402]

[22]. Hayanga JWA, Fugett J, Hayanga HK. The Affordable Care Act and access to extracorporeal membrane oxygenation as a bridge to lung transplantation in Medicaid recipients. Transpl Int 2019;32(11):1216–7. [PubMed: 31430003]

[23]. Fernando SM, Qureshi D, Tanuseputro P, Dhanani S, Guerguerian A-M, Shemie SD, et al. Long-term survival and costs following extracorporeal membrane oxygenation in critically ill children—a population-based cohort study. Critical Care 2020;24(1).

[24]. Maeda K, Ryan K, Conrad CK, Yarlagadda VV. An alternative cannulation approach for venovenous extracorporeal membrane oxygenation in children for long-term ambulatory support. J Thorac Cardiovasc Surg 2018;156(1):e13–e4. [PubMed: 29685584]

[25]. Turner DA, Cheifetz IM, Rehder KJ, Williford WL, Bonadonna D, Banuelos SJ, et al. Active rehabilitation and physical therapy during extracorporeal membrane oxygenation while awaiting lung transplantation: a practical approach. Crit Care Med 2011;39(12):2593–8. [PubMed: 21765353]

[26]. Turner DA, Rehder KJ, Bonadonna D, Gray A, Lin S, Zaas D, et al. Ambulatory ECMO as a bridge to lung transplant in a previously well pediatric patient with ARDS. Pediatrics 2014;134(2):e583–e5. [PubMed: 25049344]

[27]. Hayes MM, Fallon BP, Barbaro RP, Manusko N, Bartlett RH, Toomasian JM. Membrane Lung and Blood Pump Use During Prolonged Extracorporeal Membrane Oxygenation: Trends From 2002 to 2017. ASAIO J 2021;Online First.

[28]. Zimmermann AK, Weber N, Aebert H, Ziemer G, Wendel HP. Effect of biopassive and bioactive surface-coatings on the hemocompatibility of membrane oxygenators. Journal of Biomedical Materials Research Part B: Applied Biomaterials 2007;80B(2):433–9.

[29]. Wo Y, Brisbois EJ, Bartlett RH, Meyerhoff ME. Recent advances in thromboresistant and antimicrobial polymers for biomedical applications: just say yes to nitric oxide (NO). Biomater Sci 2016;4(8):1161–83. [PubMed: 27226170]

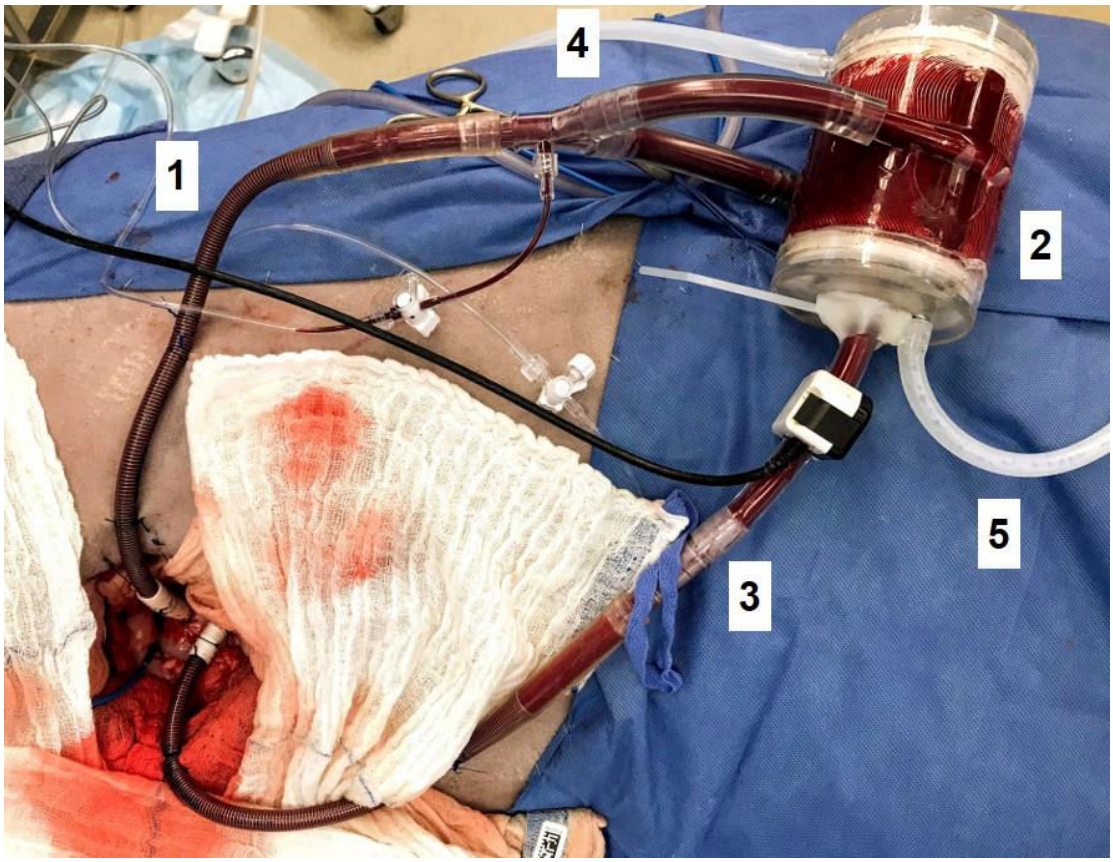

Figure 1.

Pediatric MLung circuit used for the pumpless implant experiments: 1) device inflow from the pulmonary artery, 2) Pediatric MLung, 3) device outflow to the left atrium, 4) gas line delivering sweep gas and NO to the Pediatric MLung, 5) sweep gas exhaust from which exhaust NO samples were taken. Circuit flow is clockwise in this image.

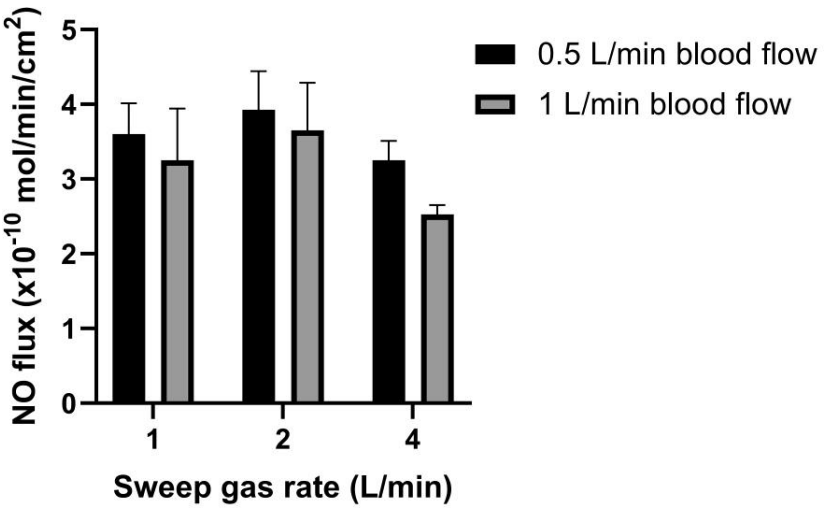

Figure 2.

Level of nitric oxide (NO) release per square centimeter of gas-exchange membrane in the Pediatric MLung as measured during NO flux experiments. Data shown are means of the 4 MLungs tested at each circuit setting (i.e., combination of blood flow and sweep gas rates). Error bars depict the standard error of the mean.

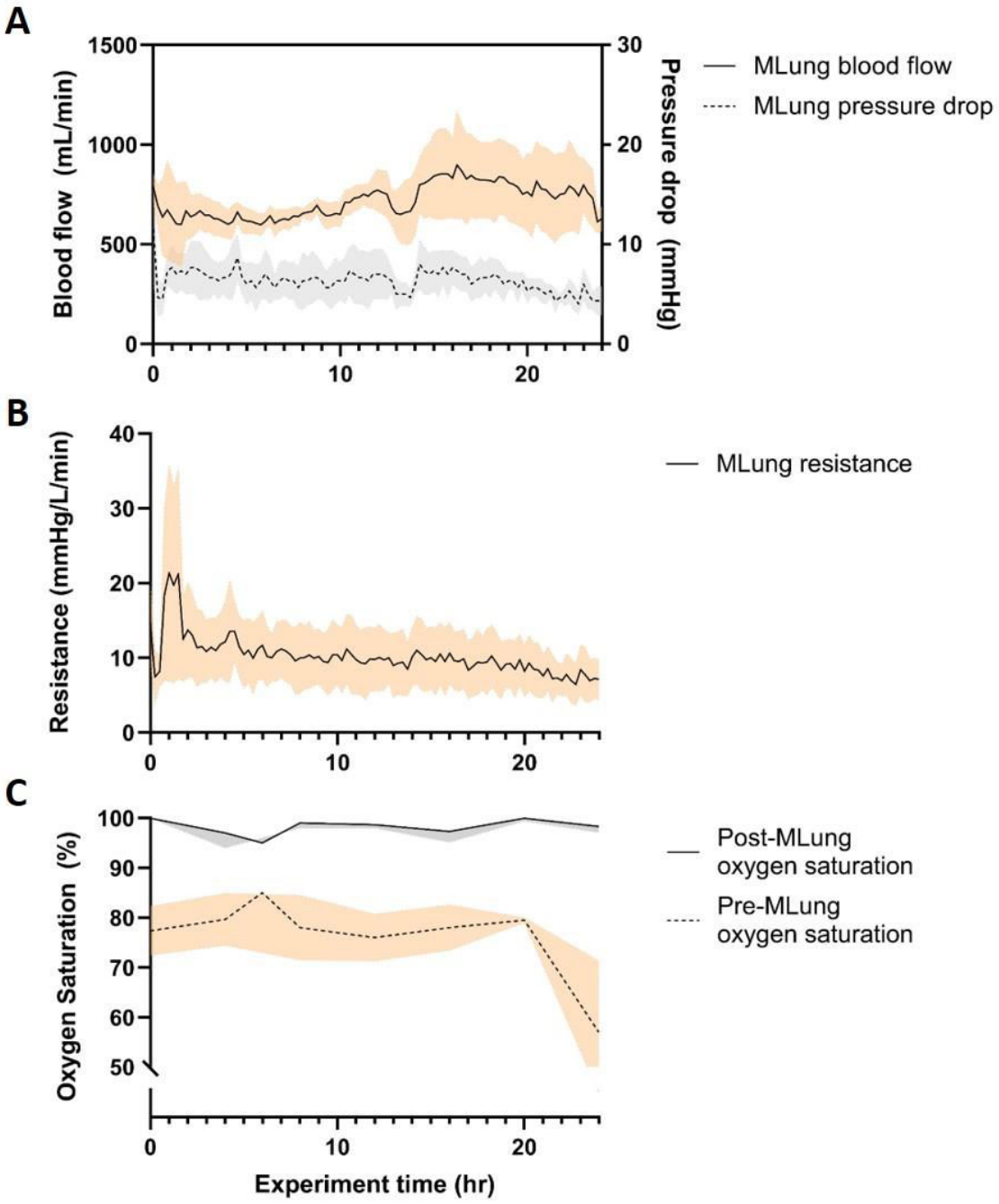

Figure 3.

Pediatric MLung performance in pumpless implant studies. Mean (A) blood flow (in mL/min) through the Pediatric MLung and pressure drop (in mmHg) across the Pediatric MLung, (B) resistance (in mmHg/L/min) across the Pediatric MLung, and (C) blood oxygen saturation pre- and post-MLung over 24 hours. Mean is calculated at each 15-minute time point for 3 sheep. Error envelopes depict standard error of the mean.

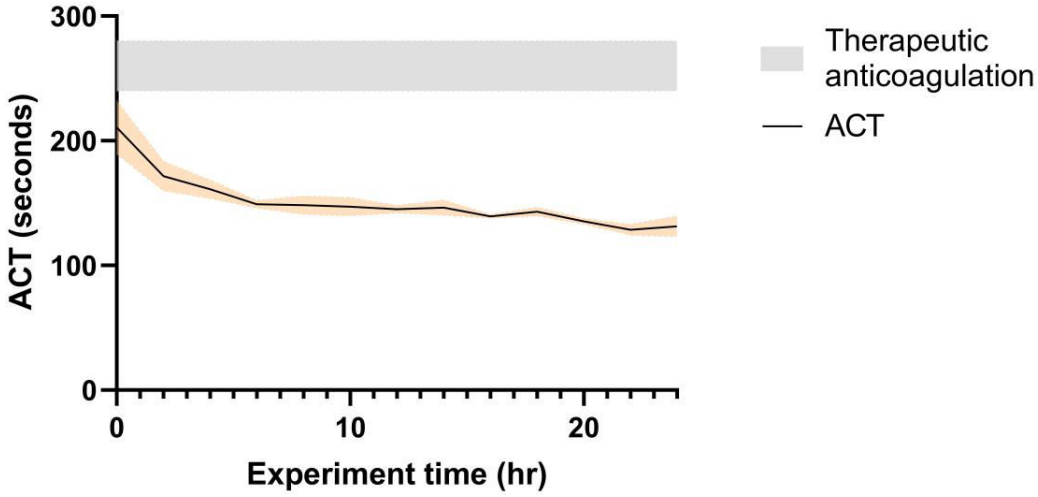

Figure 4.

Activated clotting time (ACT) across the 24-hour experiments. Heparinization occurred prior to hour 0. Data are the median ACT, measured every 2 hours, for the 3 sheep that survived 24 hours. Error envelopes indicate standard error of the mean. Shaded area depicts the target ACT range for therapeutic anticoagulation in these sheep: 240–280 seconds.

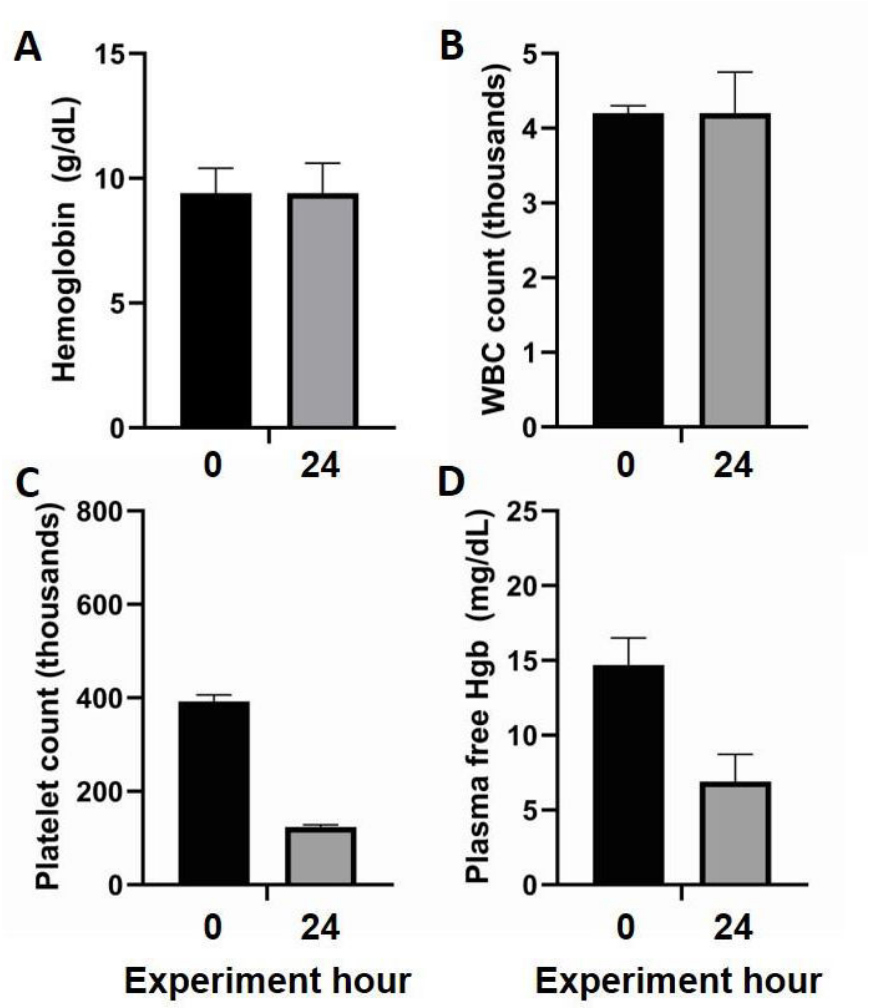

Figure 5.

A) Serum hemoglobin (in g/dL), B) white blood cell (WBC) count (in thousands/μL), C) platelet count (in thousands/μL), and D) plasma free hemoglobin (in mg/dL) at baseline (hour 0; prior to cannulation) and after 24 hours of support with the MLung and NOSA system. Data are the mean at hour 0 and hour 24 for the 3 sheep that survived 24 hours. Error bars depict the standard error of the mean.

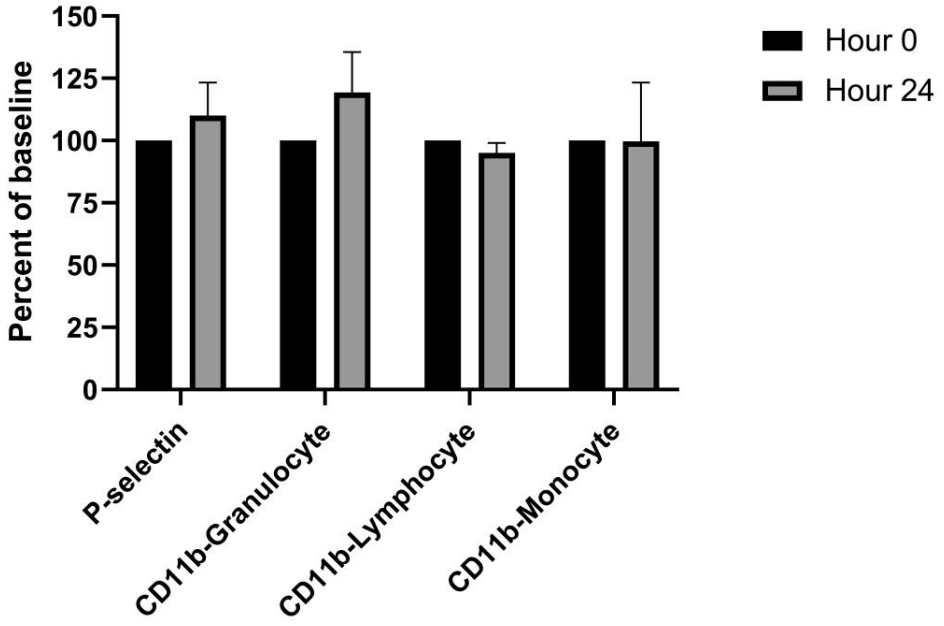

Figure 6.

Flow cytometry (cellular activation) values at baseline (hour 0; prior to cannulation) and after 24 hours of support with the MLung and NOSA system. Data are shown as a percent of the baseline expression level. Data are the mean at hour 0 and hour 24 for the 3 sheep that survived 24 hours. Error bars depict the standard error of the mean.

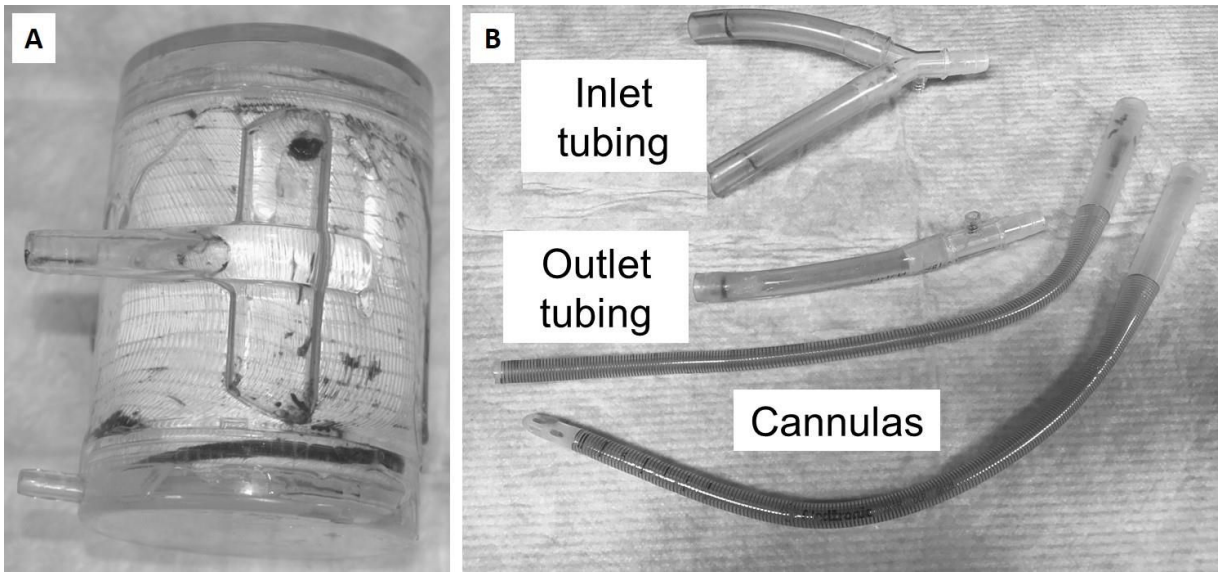

Figure 7.

A) MLung and B) circuit tubing and cannulae after 24 hours of support without anticoagulation. The circuit tubing and cannulae are coated with diazeniumdiolated dibutylhexanediamine (DBHD-N_2O_2) and argatroban.

Table 1

Characteristics of the Pediatric MLung

Characteristic	Measurement
Rated flow[1]	3 L/min (approx.)
Oxygenation rate (at rated flow)[1]	165 ± 22 mL O_2/min
Membrane surface area	0.46 m^2 (approx.)
Membrane material	polymethylpentene
Porosity	0.77
Priming volume	110 ± 5.7 mL
Target fiber length	6 cm
Diameter	8 cm
Weight, empty	0.36 kg
Weight, primed	0.47 kg

[1]Data measured during in vitro testing of the Pediatric MLung, details of which will be published separately.

Table 2

Data Collection for Pumpless Implants with NOSA

Category	Parameters	Frequency
Hemodynamics	Heart rate, arterial BP, PA pressure CO, and temperature	Monitored continuously and collected every 15 minutes
Circuit data	Device blood flow, pre and post pnssure	Monitored continuously and collected every 15 minutes
MLung gas exchange	Pre- and post-device blood gases	Every 2 hours
Acid/base balance	Arterial blood gases	Every 2 hours
Coagulation	ACT	Every 2 hours
Laboratory analysis	CBC, CMP, coagulation profile	Prior to cannulation and after 24 hours of support
Cellular activation	Flow cytometry for P-selectin, CD11b (granulocyte-, monocyte-, and lymphocyte-specific)	Prior to cannulation and after 24 hours of support
Hemolysis	Plasma free hemoglobin	Prior to cannulation and after 24 hours of support

Note: BP = blood pressure, PA = pulmonary artery, CO = cardiac output, ACT = activated clotting time, CBC = complete blood count, CMP = comprehensive metabolic panel

Table 3

Hemodynamic Data for Sheep Supported by the MLung

Vital Sign/Lab Value	Mean ± SD
Mean arterial pressure (mmHg)	67±7.7
Arterial pH	7.37±0.1
Arterial pCO_2 (mmHg)	39±5.5
Arterial pO_2 (mmHg)	191±42
HCO_3^- (mmol/L)	22±2
Arterial lactate (mmol/L)	1.8±0.5
Arterial O_2 saturation (%)	100±0.6
Mean PA pressure (mmHg)	20.1±3.4
Cardiac output (L/min)	3.8±1.8

Note: PCO_2 = partial pressure of carbon dioxide; PO_2 = partial pressure of oxygen; HCO_3^- = bicarbonate ion; PA = pulmonary artery